Progress In Electromagnetics Research C, Vol. 16, 147–160, 2010

A MEANDERED LOOP ANTENNA FOR LTE/WWAN OPERATIONS IN A SMART PHONE

C.-W. Chiu and C.-H. Chang

Department of Electronic Engineering
National Ilan University
Ilan 260, Taiwan

Y.-J. Chi

Department of Electrical Engineering
National Chiao-Tung University
Hsinchu 350, Taiwan

Abstract—This paper presents a multiband meandered loop antenna for smart phone applications. The proposed antenna which features a meandered folded-loop generates two resonance modes in the LTE/GSM bands. The current distributions of the excited resonance modes are analyzed to investigate the mode characteristic. By using a capacitively coupled feed on the backplane, the impedance bandwidth is broadened to cover LTE/WWAN bands. The simulation performed in this research used a high frequency structure simulator (HFSS) to optimally design the antenna, and a practical structure was constructed for the test. Details of the various antenna parameters are presented and discussed in this paper.

1. INTRODUCTION

LTE (Long Term Evolution) is a new high-performance air interface standard for cellular mobile communication systems. It is the last step toward the 4th generation (4G) of radio technologies designed to increase the capacity and speed of mobile telephone networks. LTE provides ultra-broadband speeds for mega multimedia applications by using a high performance antenna [1]. The frequency spectrum allocated for LTE applications ranges from 600 MHz to 3 GHz, and

Received 25 July 2010, Accepted 13 September 2010, Scheduled 26 September 2010
Corresponding author: C.-W. Chiu (alexchiu@niu.edu).

the LTE band 12–14 covers from 698 MHz to 798 MHz. For the incorporation of the LTE band with the existing cellular phone, the operating bandwidth of a handset should cover from 698 MHz to 960 MHz and from 1710 to 2690 MHz [1].

In order to include LTE700/LTE2300/LTE2500, Wong and Chen recently proposed a small-size printed loop antenna integrated with two stacked coupled-fed shorted strip monopoles for multiband operation in a mobile phone [2]. Some published papers proposed a multi-input and multi-output (MIMO) antenna configuration for LTE handset application in order to deliver ultra-broadband speeds for mega multimedia applications [3, 4]. Since the spectrum for the LTE700 system is allocated at 700 MHz bands, the operating wavelength is longer than 400 mm. The ground plane size of a typical handset (say 100 mm) is only about a quarter-wavelength. As a result, the chassis of a traditional monopole or PIFA in the handsets is a resonator. The resonating currents are spread out over the system's ground plane [5–8]. To avoid degrading of the antenna performance, a loop antenna is a good candidate for a LTE system. The performance of the loop antenna is less dependent on the ground plane, thus it is suitable for a LTE antenna design [9]. The main current distribution of the loop antenna is limited in the closed loop pattern and feed port. Therefore, handheld and head proximity influences are reduced since the current of the loop antenna on the ground plane is less than that of the PIFA or monopole [10–14].

In this paper, a compact internal antenna which operates in the LTE/GSM and PCS/UMTS/WLAN/LTE2300 bands is proposed. The antenna is a kind of folded loop which is fed by a back-coupling element connected to a microstrip transmission line [15]. A parallel monopole-like mode and a combination mode formed by loop pattern and device chassis are excited to cover the bandwidth from 698 MHz to 960 MHz. This design is easily to be implemented in a double-sided printed circuit board. The occupied geometrical space of the antenna structure measures only 60 mm × 10 mm × 6.5 mm. The proposed antenna design is described in Section 2, and a parameter study on analyzing the effect of some critical parameters is also presented. Experimental results of the proposed prototype are presented and discussed in Section 3.

2. ANTENNA DESIGN AND ANALYSIS

2.1. Antenna Design

Figure 1(a) shows the three-dimensional configuration of the proposed antenna. The antenna is mounted on a 0.8-mm thick FR4 substrate with a relative permittivity of 4.4 and a loss tangent of 0.02. The

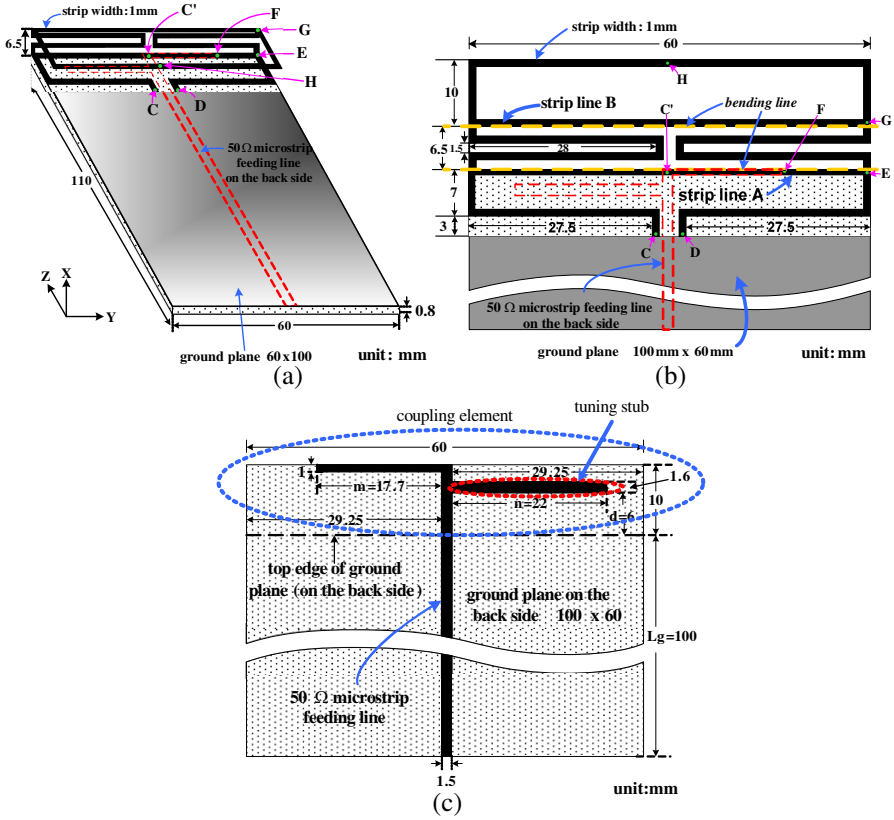

Figure 1. Geometry of the proposed antenna. (a) 3D view, (b) plan view of the front-side, and (c) plan view of the back-side.

antenna system consists of a folded loop strip and a capacitively-coupled feeding line. The loop pattern is meandered and folded to increase the electrical length but at the same time reduce the size it occupies. The total length of the folded and meandered loop strip from C to D is about 286 mm, as shown in Fig. 1(b). To excite a new resonant mode by coupling, a strip line A is arranged directly above the coupling element on the back plane. To increase electric length and support the meandered loop, a tuning strip line B is inserted into the loop. On the same side of the substrate, a copper plate which is 60 mm wide and 100 mm long is printed to act as the system ground plane of a smart phone. To broaden the impedance bandwidth, an inverted L-shape coupling element with a matching stub, as shown in Fig. 1(c), is placed on the back side and connected to the feed port. The

coupling feed scheme generates two resonance modes in the LTE/GSM band. The coupling element on the backplane is connected to a 50 ohm microstrip line with a strip width of 1.5 mm.

Figure 2(a) shows the simulated reflection coefficient for the folded loop antenna fed by the capacitively-coupled microstrip line compared with the one fed directly by a coaxial cable at point C shown in Fig. 1(b). Basically, a parallel monopole-like mode, which its current path is from point D, through E, G, to H, is excited on the loop pattern by the unbalance-fed scheme. If the antenna is fed directly, the monopole-like mode is generated on the two arms from D to H and C to H in the lower GSM band. The field of the antenna system with the direct feeding scheme is inductively coupled to the ground plane. Since the maximum magnetic field is located at the center of the ground plane, not near the rim of the conductor plane, the antenna system cannot generate a chassis wavemode. However, two resonating modes are excited when the antenna is capacitively fed on the backside of the substrate because the maximum electric field of the chassis mode is close to the rim of the ground plane. Hence, the PCB resonance mode is easily excited by capacitive coupling. As a result, the impedance bandwidth could be broadened to cover the LTE/GSM850/GSB900 bands.

Figure 2(b) shows the input impedance when the antenna is fed by the two different feed schemes. The reactance of the impedance in the low band is inductive when the antenna is fed directly by a cable at point C. This inductive reactance has a high rate of change with respect to frequency so as to limit the bandwidth; therefore, the PCB chassis mode cannot be generated. Consider the loop antenna has a back-coupled feed port. The inductive reactance is compensated by the

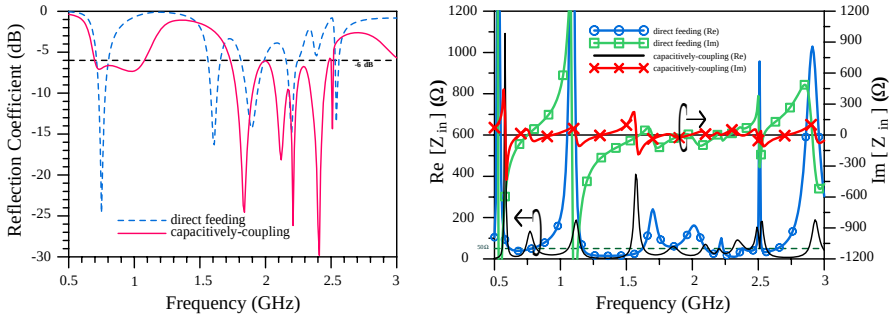

Figure 2. Simulated results of (a) the reflection coefficient and (b) the input impedance with different feed schemes.

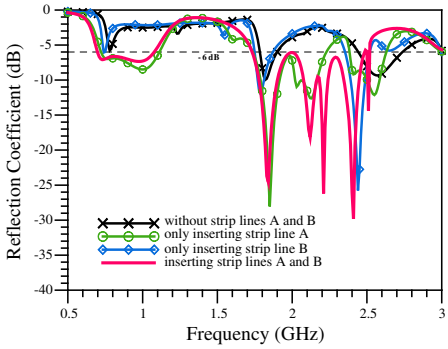

Figure 3. Simulated results of the reflection coefficient with strip lines A and B.

capacitively coupled element to form a self-complimentary impedance so as to widen the impedance bandwidth (red line).

The input signal launched from the inverted-L-shape feed line capacitively couples to strip line A. Strip line A helps to excite a new resonant mode. Fig. 3 shows the reflection coefficient for the antenna with and without strip lines A and B. A new loop mode is excited when strip line A is inserted. The new chassis-handset combination, which is generated from point C', through F, E, G to H and C', is supported by the coupled structure with strip line A, as Fig. 1(b) shows. On the other hand, a parasitic line B is inserted into the loop to increase the electrical length of the lowest resonance frequency and support the folded loop. When inserting the strip lines A and B, this study finds that the bandwidth is broadened because two modes are generated in the low GSM band.

2.2. Current Distribution

The surface current distribution on the conductor strip confirms the mode characteristic. Fig. 4 shows the vector current distributions at 720 and 990 MHz. The current behavior demonstrates that the monopole-like mode creates the resonance at 720 MHz and the antenna-chassis combination mode at 990 MHz, respectively. These results are simulated by a commercial electromagnetic simulation tool, HFSS. The strip ends of the loop antenna structure symmetrically terminate to the ground plane. The currents on both sides of the loop are of the same phase at 720 MHz with respect to the central feed line, as Fig. 4(a) shows. Thus, the antenna behaves like two parallel folded monopoles at 720 MHz. The quarter wavelength at 720 MHz is calculated to be around 104 mm but the meander length of one arm, as shown in

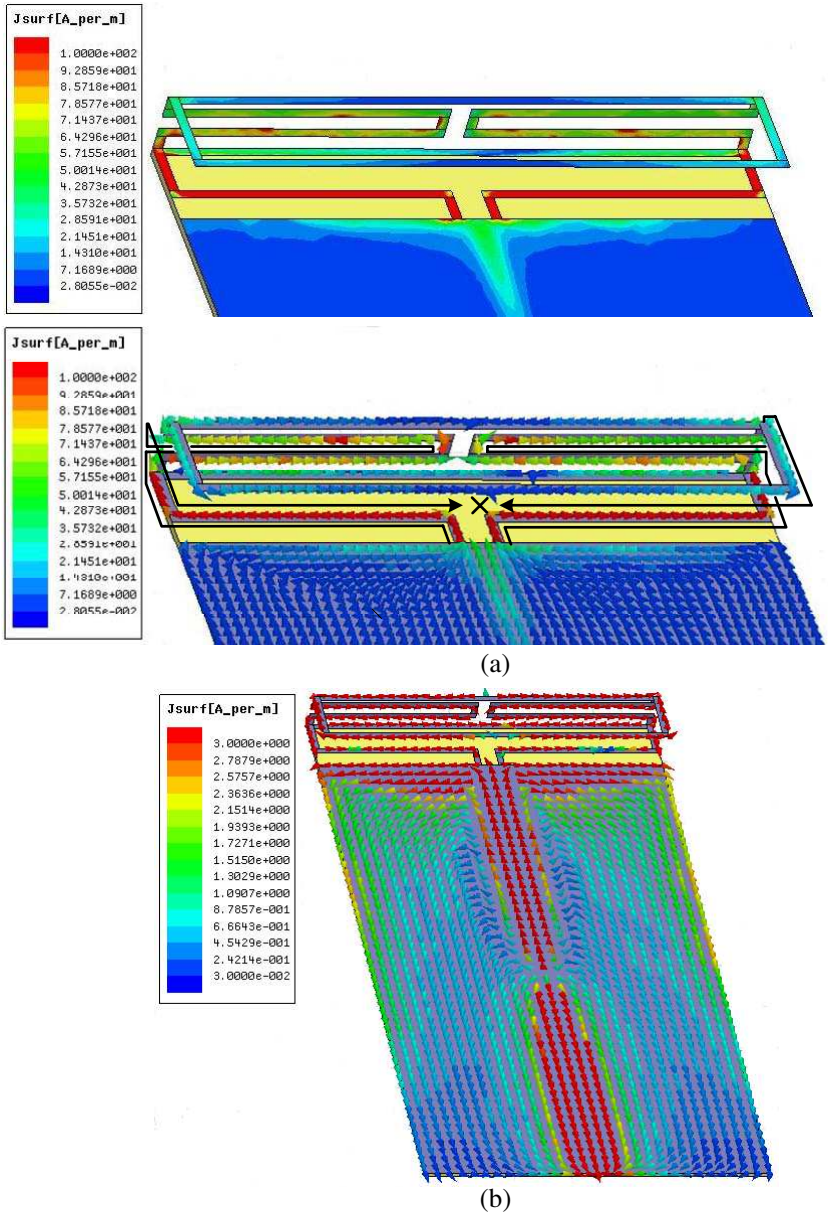

Figure 4. Simulated vector current distributions and surface current densities. (a) 720 MHz, (b) 990 MHz.

Fig. 1(b), is around 141.5 mm. The physical length of the wavelength of the monopole-like mode is longer than the electrical length due to fold and meander. The monopole-like mode can also be verified by the radiation patterns discussed in Section 3, where E_Θ in the x-y plane is basically omni-directional.

The current behavior in Fig. 4(b) shows that the antenna-chassis combination mode is excited at 990 MHz. Since the proposed antenna has an unbalanced feeding scheme, the currents are generated on the groundplane, and therefore, the ground plane is operated as a part of a radiator. Since the ground length is smaller than half-wave length below 1 GHz, the resonance mode at 990 MHz uses the printed circuit board of the mobile terminal as part of the antenna. The characteristic wave modes of the PCB conductor have contribution on the combined radiation behavior of the PCB and the loop element. The radiation mode is characterized as the combination of the handset antenna and the PCB conductor [16]. The current distribution at 990 MHz shows that it doesn't form complete resonance current path in the loop pattern. The antenna element dominantly acts as a coupling element at 990 MHz. Therefore, the antenna system can be modeled as a dual-resonant circuit [16]. The radiation mode due to the groundplane resonance enhances the bandwidth when the antenna system is properly designed [7]. Fig. 5 shows the effect of ground length Lg on the antenna performance, and observations showed larger effects on the resonance modes in the low band. The longer the length, the greater the bandwidth [7, 16].

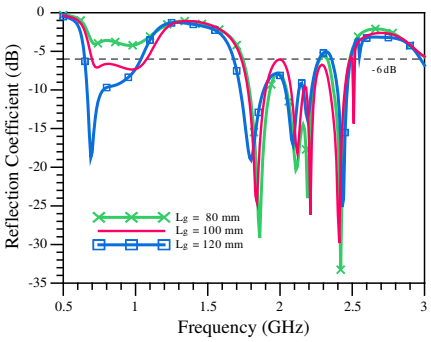

Figure 5. Simulated results as a function of length L_g (system ground plane length).

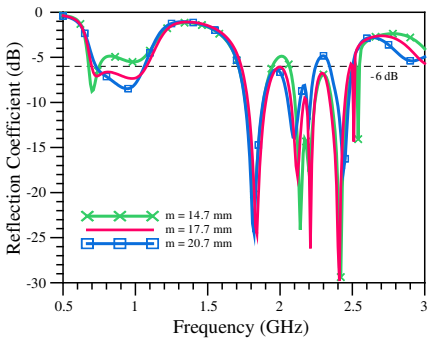

Figure 6. Simulated results as a function of length m.

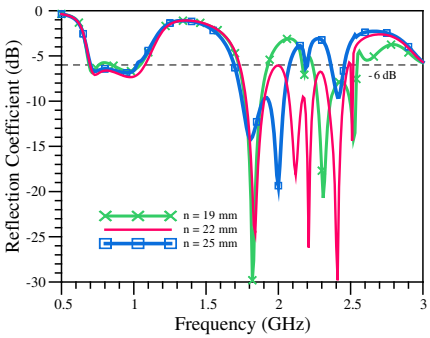

Figure 7. Simulated results as a function of length n of the tuning stub.

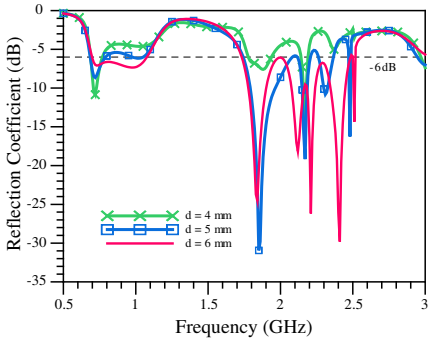

Figure 8. Simulated results as a function of distance d of the tuning stub.

2.3. Parametric Analysis

To obtain better impedance matching, an inverted L-shape coupling element with a tuning stub is connected to the feeding microstrip line on the back plane. The design of the coupling element is a critical factor. This research conducted a parametric study on the length m and the stub length n shown in Fig. 1(c). When the parameter m varies between 14.7 to 24.7 mm or the parameter n varies from 19 to 25 mm, the rest of the dimensions of the antenna remain the same as shown in Fig. 1. Fig. 6 shows the simulation reflection coefficient as a function of length m. Length m plays an important role in exciting the second mode in the low band. The variation in length has a substantial influence on the impedance matching in the design bands. Fig. 7 shows the simulation reflection coefficient as a function of stub length n. The findings show that the stub length n has a larger effect in the higher band. When the length is tuned to about 22 mm, the bandwidths in the low band and the higher band achieve the bandwidth requirement of -6 dB. Fig. 8 shows the simulation reflection coefficient as a function of d which is the distance from the ground plane edge to the tuning stub shown in Fig. 1(c). When distance d is fixed at 6 mm, the impedances are well matched in the higher band.

3. RESULTS OF THE PROPOSED ANTENNA

The proposed antenna was constructed for testing purposes. The measurements were performed using an Agilent E5071B network analyzer. Fig. 9 shows the measured and simulated reflection

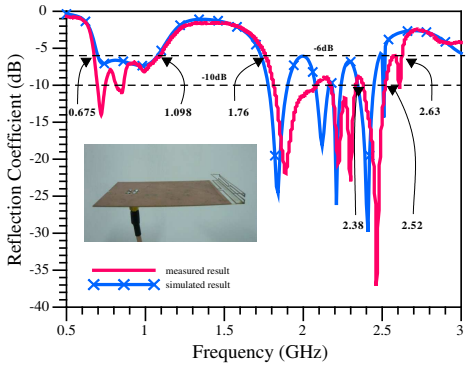

Figure 9. Measured results compared with simulation results.

coefficient of the proposed antenna. The simulated results were obtained using Ansoft HFSS. There was a good agreement between the measurement and simulation below 1.8 GHz. The finding shows that the achieved bandwidth covers the LTE/GSM850/GSM900 band and PCS/UMTS/WLAN/LTE2300. In the low band, the achieved bandwidth with reflection coefficient better than −6 dB was 423 MHz (675–1098 MHz) and in the high band it was 870 MHz (1760–2630 MHz).

Figure 10 shows the measured and simulated radiation patterns of the proposed antenna on the XY plane. The radiation-pattern and gain measurements were performed in the anechoic chamber of SGS Ltd. Company in Taiwan. The radiation patterns E_Θ are nearly omni-directional in the xy-plane. These features are desirable characteristics for mobile phones. Fig. 11 shows the measured peak gains and radiation efficiencies. The peak gains and the radiation efficiencies were measured using the ETS-Lindgren model AMS-8500 antenna measurement system and the 3164-08 open boundary quad-ridged horn antenna, respectively. The measured antenna gain over the low band varied from around 1.5–3.0 dBi and the radiation efficiency was higher than 50%. The measured antenna gain for the higher band varied around 1–4.2 dBi and the radiation efficiency was larger than 50%, ranging from 1.8 to 2.5 GHz. Since the connecting semi-rigid coaxial cable (about 30 cm) between the DUT and the testing system of SGS is not wrapped by a choke or a ferrite bead, the connecting cable used in the measurement acts as a radiator in the lower band (below 1 GHz) due to the currents traveling on its outer face [17]. The additional radiation from the outer conductor of the cable has some impact on the gain. Therefore, the measured gain is larger than that

of ordinary monopoles in the lower band.

The specific absorption rate (SAR) of the proposed antenna was studied using the FEKO simulation software [18]. Fig. 12 shows the simulation model with the antenna placed at the cheek position near the phantom. The phantom of the head model used in SAR computation is a specific anthropomorphic mannequin (SAM) defined by the IEEE Standards Coordinating Committee 34 [19]. The separation distance between the system ground plane and the earpiece of the SAR phantom head is 5 mm. The tilted angle between the center

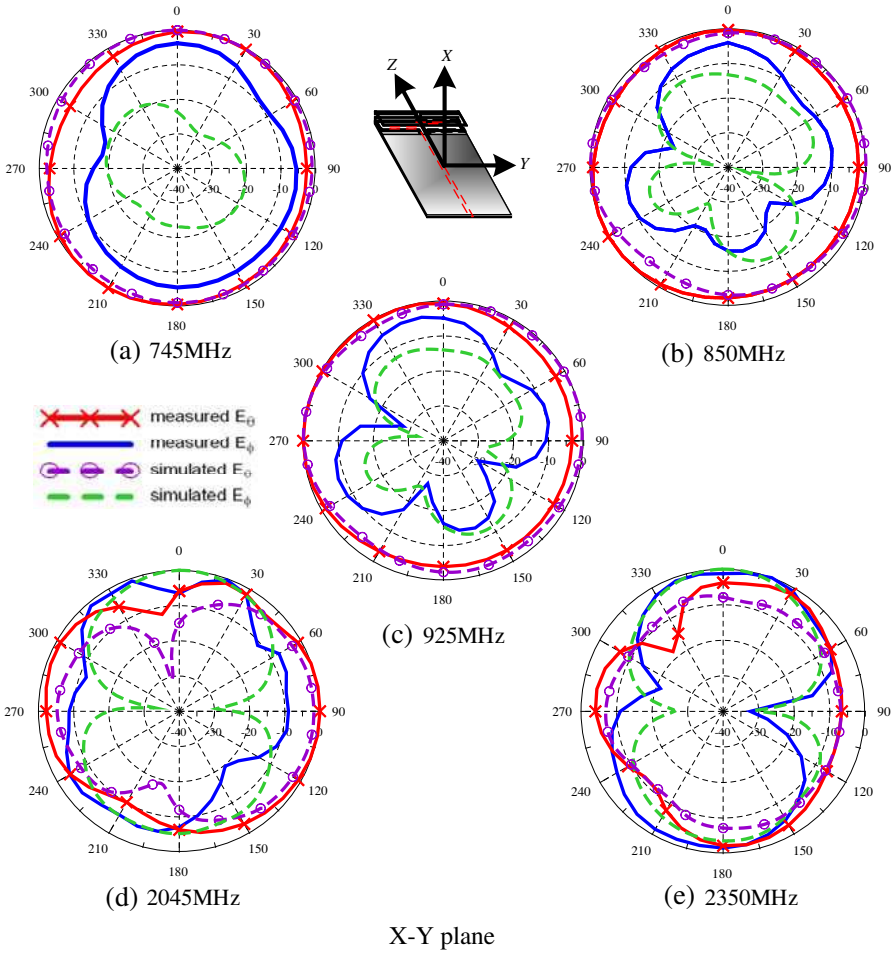

Figure 10. Measured and simulated radiation patterns at 745 MHz, 850 MHz, 925 MHz, 2.045 GHz, and 2.35 GHz, respectively.

line of the printed circuit board and the vertical line of the phantom is 63°. The antenna is placed at the top edge of the system ground plane or at the bottom position (rotating 180°). The testing power is 24 dBm (0.25 W) for the GSM850/GSM900/UMTS bands, while the testing power is 20.8 dBm (0.121 W) for the DCS/PCS bands. Table 1 lists the simulated 1-g average SARs at the transmitting frequencies of 836.6, 914.8, 1747, 1880, and 1950 MHz. The finding shows that the SAR at the bottom position is lower than that at the top position owing to the larger distance to the cheek. It seems that placing the antenna at the bottom edge is more promising for practical mobile phone applications.

Table 1. Simulated 1-g average SAR(W/kg) at GSM850/GSM900-/DCS/PCS/UMTS bands.

Band	GSM850	GSM900	DCS	PCS	UMTS
Frequency (MHz)	$f = 836.6$	$f = 914.8$	$f = 1747$	$f = 1880$	$f = 1950$
At the top (W/kg)	1.866	1.887	1.734	1.712	3.281
At the bottom (W/kg)	1.177	1.149	0.739	0.891	1.458

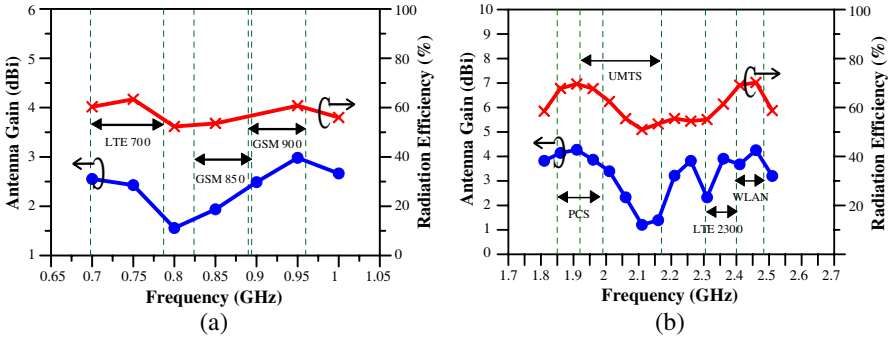

Figure 11. Measured peak gain and radiation efficiency, (a) in the low band and (b) in the higher band.

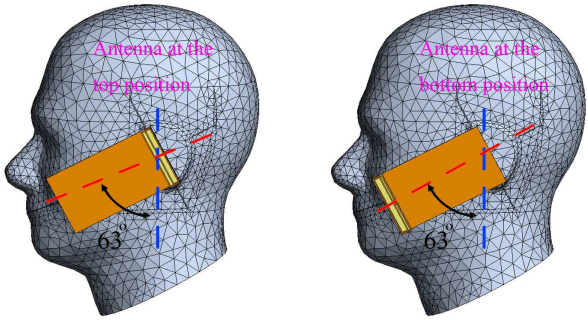

Figure 12. Simulation model with the proposed antenna for the SAR analysis.

4. CONCLUSION

This paper proposes a folded and meandered loop antenna for smart phone applications. By using a capacitively coupled feed on the back plane, two resonance modes excited on the meandered loop pattern and the ground plane have been demonstrated to achieve wideband in the lower band. The parametric study on the coupling element was performed to optimally design the folded loop antenna. The measured results on the constructed antenna were presented to validate the proposed design. The achieved bandwidth ranges from 675 to 1098 MHz and 1760 to 2630 MHz, and the measured results indicate that they cover LTE and WWAN bands. Since the proposed loop antenna is designed to include the new emerging LTE700/LTE2300/LTE2500 bands, it is very suitable for the use in the 4G smart phone.

ACKNOWLEDGMENT

We are grateful to the National Center for High-performance Computing for the HFSS computer time and use of facilities. Also, the authors would like to thank Mr. Yu-Chou Chuang and Mr. Cheng-Chang Chen, Bureau of Standards, Metrology and Inspection, M.O.E.A, Taiwan, for their help in the SAR simulation using the FEKO simulation tool.

REFERENCES

1. Sesia, S., I. Toufik, and M. Baker, *LTE — The UMTS Long Term Evolution: From Theory to Practice*, Wiley, Chichester, UK, 2009.
2. Wong, K. L. and W. Y. Chen, "Small-size printed loo-type antenna integrated with two stacked coupled-fed shorted strip monopoles for eight-band LTE/GSM/UMTS operation in the mobile," *Microwave and Optical Technology Letters*, Vol. 52, No. 7, 1471–1476, Jul. 2010.
3. Chaudhury, S. K., H. J. Chaloupka, and A. Ziroff, "Novel MIMO antennas for mobile terminal," *Proceedings of the 1st European Wireless Technology Conference*, 330–333, Amsterdam, Netherlands, Oct. 2008.
4. Bhatti, R. A., S. Yi, and S. O. Park, "Compact antenna array with port decoupling for LTE-standardized mobile phones," *IEEE Antennas and Wireless Propagation Letters*, Vol. 8, 1430–1433, 2009.
5. Abedin, M. F. and M. Ali, "Modifying the ground plane and its effect on planar inverted-F antennas (PIFAs) for mobile phone handsets," *IEEE Antennas and Wireless Propagation Letters*, Vol. 2, 226–229, 2003.
6. Anguera, J., I. Sanz, A. Sanz, A. Condes, D. Gala, C. Puente, and J. Soler, "Enhancing the performance of handset antennas by means of groundplane design," *IEEE International Workshop on Antenna Technology: Small Antennas and Novel Metamaterials (IWAT)*, 29–32, New York, USA, Mar. 2006.
7. Cabedo, A., J. Anguera, C. Picher, M. Ribó, and C. Puente, "Multi-band handset antenna combining PIFA, slots, and ground plane modes," *IEEE Transactions on Antennas and Propagation*, Vol. 57, No. 9, 2526–2533, Sep. 2009.
8. Picher, C., J. Anguera, A. Cabedo, C. Puente, and S. Kahng, "Multiband handset antenna using slots on the ground plane: Considerations to facilitate the integration of the feeding transmission line," *Progress In Electromagnetics Research C*, Vol. 7, 95–109, 2009.
9. Lin, C. I. and K. L. Wong, "Internal meandered loop antenna for GSM/DCS/PCS multiband operation in a mobile phone with the user's hand," *Microwave and Optical Technology Letters*, Vol. 49, No. 4, 759–765, Apr. 2007.
10. Chi, Y. W. and K. L. Wong, "Internal compact dual-band printed loop antenna for mobile phone application," *IEEE Transactions on Antennas and Propagation*, Vol. 55, No. 5, 1457–1462,

May 2007.

11. Wong, K. L. and C. H. Huang, "Printed loop antenna with a perpendicular feed for penta-band mobile phone application," *IEEE Transactions on Antennas and Propagation*, Vol. 56, No. 7, 2138–2141, Jul. 2008.
12. Chi, Y. W. and K.-L. Wong, "Compact multiband folded loop chip antenna for small-size mobile phone," *IEEE Transactions on Antennas and Propagation*, Vol. 56, No. 12, 3797–3803, Dec. 2008.
13. Chiu, C. W., C. H. Chang, and Y. J. Chi, "Multiband folded loop antenna for smart phones," *Progress In Electromagnetics Research*, Vol. 103, 123–136, 2010.
14. Chiu, C. W. and Y. J. Chi, "Printed loop antenna with a U-shaped tuning element for hepta-band laptop applications," *IEEE Transactions on Antennas and Propagation*, Vol. 58, No. 11, Nov. 2010.
15. Li, W. Y. and K. L. Wong, "Seven-band surface-mount loop antenna with a capacitively coupled feed for mobile phone application," *Microwave and Optical Technology Letters*, Vol. 51, No. 1, 81–88, Jan. 2009.
16. Vainikainen, P., J. Ollikainen, O. Kivekas, and K. Kelander, "Resonator-based analysis of the combination of mobile handset antenna and chassis," *IEEE Transactions on Antennas and Propagation*, Vol. 50, No. 10, 1433–1444, Oct. 2002.
17. Chen, Z. N., N. T. Yang, Y. X. Guo, and M. Y. W. Chia, "An investigation into measurement of handset antennas," *IEEE Trans. Instrumentation and Measurement*, Vol. 54, No. 3, 1100–1110, Mar. 2005.
18. FEKO, EM Software & Systems — S.A. (Pty) Ltd. (EMSS), [Online], available: http://www.feko.info.
19. Beard, B. B. and W. Kainz, "Review and standardization of cell phone exposure calculations using the SAM phantom and anatomically correct head models," *Biomed. Eng. Online*, Vol. 3, 34, Oct. 13, 2004.